IL-2 enhances effector function but suppresses follicular localization of CD8$^+$ T cells in chronic infection

Yaping Chen[1,2,9], Pengcheng Zhou[3,4,6,9*], Patrick Marc Gubser[5], Yew Ann Leong[1], Jing He[6], Yunbo Wei[7], Fadzai Victor Makota[3], Mehrdad Pazhouhandeh[4], Ting Zheng[3,7], Joseph Yunis[3,4,8], Zhanguo Li[6], Axel Kallies[5*], Di Yu[1,3,4,8,10*]

1 Department of Biochemistry, School of Biomedical Sciences, Biomedical Discovery Institute, Monash University, Clayton, Victoria, Australia

2 Oujiang Laboratory (Zhejiang Lab for Regenerative Medicine, Vision and Brain Health), Wenzhou, Zhejiang, P.R. China

3 Immunology and Infectious Disease Division, John Curtin School of Medical Research, The Australian National University, Canberra, Australian Capital Territory, Australia

4 Frazer Institute, Faculty of Medicine, The University of Queensland, Brisbane, Queensland, Australia

5 The Peter Doherty Institute for Infection and Immunity, Department of Microbiology and Immunology, The University of Melbourne, Parkville, Victoria, Australia

6 Department of Rheumatology & Immunology, Peking University People's Hospital, Beijing, China

7 Laboratory of Immunology for Environment and Health, Shandong Analysis and Test Center, Qilu University of Technology (Shandong Academy of Sciences), Jinan, Shandong, China

8 Ian Frazer Centre for Children’s Immunotherapy Research, Children’s Health Research Centre, Faculty of Medicine, The University of Queensland, Brisbane, Queensland, Australia

9 These authors contributed equally

10 Lead corresponding author

*Correspondence:

D.Y. (di.yu@uq.edu.au)

A.K. (axel.kallies@unimelb.edu.au)

P.Z. (pzhou@rockefeller.edu)

Summary

Cytotoxic $CD8^+$ T cells, essential in combating viral infections and cancer, become dysfunctional from prolonged antigen exposure. Precursors of exhausted T (T_{PEX}) cells are pivotal in sustaining immune responses in chronic diseases and mediating immunotherapy efficacy. They also control viral infection within B-cell follicles, facilitated by CXCR5 expression. How cytokines regulate T_{PEX} cell fate and follicular entry is not well understood. We reveal that IL-2 treatment enhances $CD8^+$ T cell effector functions in chronic LCMV infection but hinders $CXCR5^+$ T_{PEX} cell formation and infection control within B-cell follicles. Mechanistically, IL-2 suppresses T_{PEX} cell differentiation in a STAT5 and BLIMP1-dependent manner. Using an IL-2 fusion protein targeting CD122, we shifted the differentiation towards $CX3CR1^+$ T cells with increased effector function. Clinical observations with low-dose IL-2 in autoimmune disease confirmed IL-2's inhibitory effect on $CXCR5^+$ T_{PEX} cells, underscoring IL-2's crucial regulatory role and therapeutic potential in modulating T_{PEX} and effector T cell generation.

Keywords:

Interleukin-2, LCMV, follicular infection, T_{PEX}, CXCR5, STAT5

INTRODUCTION

$CD8^+$ T cells play a critical role in eliminating virally infected and malignant cells. In chronic infection and cancer, antigen-specific $CD8^+$ T cells persistently exposed to antigen gradually reduce their ability to produce effector cytokines and proliferative capacity. This process is paralleled by the upregulation of inhibitory receptors or checkpoints such as programmed cell death protein 1 (PD-1), T cell immunoglobulin and mucin domain 3 (TIM-3) and lymphocyte-activation gene 3 (LAG3). Although such cellular reprogramming is necessary to restrain $CD8^+$ T cells-mediated immunopathology, reduced functionality in $CD8^+$ T cells impairs the clearance of infection or prevention of tumor growth. This process is referred to as T cell exhaustion (Blank et al., 2019; Hashimoto et al., 2018; McLane et al., 2019).

PD-1^+ exhausted $CD8^+$ T cells are heterogenous and contain a population of cells known as progenitors or precursors of exhausted T (T_{PEX}) cells. These cells retain the capacity to self-renew while also giving rise to exhausted effector T (T_{EX}) cells as we and others have shown (He et al., 2016b; Im et al., 2016; Leong et al., 2016; Utzschneider et al., 2016; Wu et al., 2016). T_{PEX} cells also mediate the response to immune checkpoint blockade (ICB) therapies that inhibit PD-1/PD-Ligand 1 (PD-L1) interactions and thus amplify anti-viral and anti-tumor immunity in mice and humans (Eberhardt et al., 2021; Huang et al., 2022; Im et al., 2016; Siddiqui et al., 2019; Utzschneider et al., 2016). T_{PEX} cells express the chemokine receptor CXCR5, which facilitates their migration to B-cell follicles where they contribute to the suppression of infection (He et al., 2016b; Leong et al., 2016). This is important as B-cell follicles act as reservoirs for certain viruses, such as Epstein–Barr virus (EBV) in memory B cells and Human Immunodeficiency Virus (HIV) in follicular helper T (T_{FH}) cells (Collins et al., 2023; Leong et al., 2016; Mylvaganam et al., 2017; Petrovas et al., 2017). Therefore, CXCR5-expressing T_{PEX} cells are critical in suppressing the infection in B-cell follicles (Yu and Ye, 2018).

T cell exhaustion is controlled by a network of transcriptional regulators induced by T cell receptor (TCR) stimulation-induced transcription factors, in particular NFATC1, TOX and IRF4 drive the sustained expression of inhibitory receptors and contribute to the downregulation of effector function (Alfei et al., 2019; Khan et al., 2019; Man et al., 2017;

Martinez et al., 2015; Scott et al., 2019; Seo et al., 2019; Yao et al., 2019). The generation and maintenance of T_{PEX} cells, on the other hand, are specifically controlled by transcription factors such as TCF1, MYB, ID3 and BCL6 while T_{EX} cells differentiation is promoted by BLIMP1(Gautam et al., 2019; He et al., 2016b; Im et al., 2016; Leong et al., 2016; Tsui et al., 2022; Utzschneider et al., 2016; Wu et al., 2016). However, extracellular signals that regulate T_{PEX} and T_{EX} cell differentiation and maintenance are less understood. We and others have shown that TGFβ plays a key role in maintaining T_{PEX} cell function and identity (Gabriel et al., 2021; Hu et al., 2022; Ma et al., 2022). Furthermore, both T_{FH} cells-derived cytokine interleukin-21 (IL-21) and the alarmin IL-33 are necessary to maintain T_{PEX} cells and sustain effector $CD8^+$ T cell function in chronic infection (Marx et al., 2023; Yu et al., 2022; Zander et al., 2022). Finally, IL-2, in combination with ICB, was shown to direct T_{PEX} cells to generate transitory effector $CD8^+$ T cells and improve antiviral and antitumor activities (Codarri Deak et al., 2022; Hashimoto et al., 2022; Ren et al., 2022; Tichet et al., 2023; West et al., 2013). However, the precise function of IL-2 in regulating T cell exhaustion is not fully understood.

To better understand how IL-2 regulates T_{PEX} cell differentiation and function, we investigated the impact and molecular mechanisms of treatment with IL-2 or a clinical-grade IL-2 fusion protein specifically targeting the IL-2 receptor β chain (CD122) in chronic LCMV infection. IL-2 treatment increased the generation of CX3CR1+ T_{EX} cells with enhanced effector function without disrupting the self-renewal capacity of T_{PEX} cells both in mouse and human. At the same time, IL-2 treatment resulted in downregulation of CXCR5 expression on T_{PEX} cells, their exclusion from B-cell follicles and impaired viral clearance from these sites. Furthermore, increased IL-2 signaling during the early stages of the immune response strongly suppressed T_{PEX} cell generation. Mechanistically, IL-2 exerted its effects in a STAT5- and BLIMP1-dependent manner. Overall, our data show that IL-2 treatment can broadly modulate the balance between effector T cells and T_{PEX} cells and excert differential effects on viral clearance.

RESULTS

IL-2 treatment promotes $CD8^+$ T effector expansion during chronic infection

IL-2 is an approved immunotherapeutic agent for cancer (Dutcher et al., 2014). It's precise mechanism of action is not fully understood. To elucidate how IL-2 affects exhausted $CD8^+$ T cell maintenance and function, wild-type C57BL/6 mice were infected with LCMV Docile (10^6 plaque-forming units, PFU), which induces chronic infection and robust T cell exhaustion. Mice were treated with PBS or low-to-medium dose of recombinant human IL-2 (30,000 international units, IU (Blattman et al., 2003; He et al., 2016a; West et al., 2013)) daily from day 10 to 14 post-infection before analysis on day 15 (**Figure 1A**). IL-2 treatment elevated $CD8^+$ T cell numbers and increased $CD8^+/CD4^+$ T cell ratios (**Figure 1B**). Furthermore, numbers of activated $CD8^+$ T cells ($CD44^{high}CD62L^-$) and their effector function as measured by Granzyme B expression were significantly enhanced by IL-2 treatment (**Figure 1C, D**). In agreement with previous studies (Blattman et al., 2003; Zhou et al., 2021), we found that IL-2 treatment significantly increased both the frequencies and numbers of LCMV-specific $CD8^+$ T cells as measured by staining with H-$2D^b$ LCMV GP_{33} tetramers (**Figure 1E**). We did not observe an expansion of regulatory (T_{REG}) cells by this dose of IL-2 treatment (data not shown), presumably due to the high numbers of activated effector T cells (Humblet-Baron et al., 2016; Zhou et al., 2021). We next examined the impact of IL-2 treatment on the generation of $TCF1^+CXCR5^+$ T_{PEX} and $TCF1^-CXCR5^-$ T_{EX} cells. IL-2 treatment increased the total numbers of T_{EX} cells by more than two-fold (**Figure 1F**). In contrast, IL-2 treatment reduced the frequencies of T_{PEX} cells within GP_{33} tetramer$^+$ $CD8^+$ T cells by more than two-fold although their numbers remained largely unchanged (**Figure 1F**). Overall, IL-2 treatment enhanced effector T cell expansion in chronic infection.

IL-2 alters tissue localization of $CD8^+$ T cells and viral reservoirs in chronic infection

Previous studies reported that a short period of IL-2 treatment, despite enhancing $CD8^+$ T effector function, was insufficient to significantly reduce viral loads (Blattman et al., 2003; Zhou et al., 2021). LCMV preferentially infects myeloid cells expressing high levels of α-Dystroglycan (α-DG), the cellular receptor for LCMV (Kunz et al., 2001; Oldstone and Campbell, 2011), but it also infects lymphocytes including $CD4^+$ T cells (Leong et al., 2016). Immunofluorescent microscopy of splenic tissue using the antibody (VL4) to LCMV

nucleoprotein revealed that IL-2 treatment resulted in an altered distribution of VL4$^+$ LCMV reservoirs towards B220$^+$ B-cell follicles (**Figure 2A**). To examine whether IL-2 treatment influenced the distribution of virus in the B-cell follicle and the T-cell zone, we deployed a flow cytometry-based method previously developed (Leong et al., 2016). Treatment with IL-2, in a dose-dependent manner, reduced numbers of virus-infected CXCR5^{low}CD44$^+$ non-T_{FH} effector CD4$^+$ T cells, which primarily reside in the T-cell zone, whereas the numbers of virally infected CXCR5^{high}CD44$^+$ T_{FH} cells, which mostly reside in B-cell follicles, remained unchanged. As a consequence, the LCMV reservoir was biased towards the B-cell follicle, indicated by a two-fold increase in the ratio of infected T_{FH}/non-T_{FH} cells at the highest dose of IL-2 treatment (**Figure 2B**).

T_{PEX} cells that express CXCR5 have access to the B-cell follicle and contribute to viral control (Collins et al., 2023; Leong et al., 2016; Petrovas et al., 2017). The altered distribution of LCMV reservoirs, however, suggested that IL-2 treatment prevents access of CD8$^+$ T cells to B-cell follicles. Indeed, IL-2 treatment significantly reduced CXCR5 expression on T_{PEX} cells (**Figure 2C**). In line with this observation, immunofluorescent imaging of splenic tissue sections revealed a drastic reduction of CD8$^+$ T cells in the B-cell follicles in IL-2-treated mice compared with that of PBS-treated control mice (**Figure 2D**).

Systemic administration of IL-2 may control CD8$^+$ T cell activation and differentiation directly or indirectly. We therefore assessed the direct impact of IL-2 *in vitro*. Stimulation of human CD8$^+$ T cells with anti-CD3/CD28 and cytokines TGFβ, IL-12, and IL-23 was shown to promote CXCR5 expression (Mylvaganam et al., 2017). In lijne with that observation, we and others found that TGFβ supported T_{PEX} cell generation and maintenance (Gabriel et al., 2021; Hu et al., 2022; Ma et al., 2022). We therefore optimized a culture condition whereby naïve mouse OT-I CD8$^+$ T cells that carry a transgenic TCR-specific to ovalbumin (OVA) antigen were stimulated with splenocytes pulsed with SIINFEKL peptide in the presence or absence of TGFβ and IL-6, with or without IL-2. The combination of TGFβ and IL-6 induced CXCR5 expression on OT-I T cells. In contrast, the addition of IL-2 in the culture diminished CXCR5 expression by about three-fold (**Figure 2E**). Overall, these results suggest that IL-2 induces signaling that favors the generation of CXCR5$^-$ T_{EX} cells over CXCR5$^+$ T_{PEX} cells in CD8 T cells.

An IL-2-STAT5-BLIMP1 axis regulates the balance of effector and T_{PEX} generation

To better understand the impact of IL-2 on T_{PEX} and T_{EX} cell generation, we performed Gene Set Enrichment Analysis (GSEA) of CXCR5$^+$ T_{PEX} cells compared to CXCR5$^-$ T_{EX} cells (Leong et al., 2016). This analysis indicated downregulation of IL-2-STAT5 signaling in CXCR5$^+$ T_{PEX} cells (**Suppl. Figure 1A**), suggesting that IL-2 negatively impacts the generation or function of CXCR5$^+$ T_{PEX} cells. The IL-2 receptor is a heterotrimeric protein complex composed of three subunits: the α subunit CD25 encoded by *Il2ra*, the β subunit CD122 encoded by *Il2rb*, and the common γ chain CD132 encoded by *Il2rg* (Boyman and Sprent, 2012). Transcriptomic analysis indicated that *Il2ra* and *Il2rb* were lower in CXCR5$^+$ T_{PEX} population, whereas *Il7r* was higher, compared with CXCR5$^-$ T_{EX} cells (**Suppl. Figure 1B,C**). Flow cytometric analysis showed that the expression of CD122 on CXCR5$^+$ T_{PEX} was significantly lower than that on CXCR5$^-$ T_{EX} cells, while CD25 protein was minimally expressed on both populations (**Figure 3A**). Notably, the treatment of IL-2 in mice with LCMV infection pronouncedly increased CD122 expression and modestly increased CD25 expression on T_{PEX} cells, whereas such effects were not observed in T_{EX} cells (**Figure 3B** and **Suppl. Figure 1D**).

The phosphorylation of STAT5 (pSTAT5) is a major signaling event induced by IL-2 (Boyman and Sprent, 2012). IL-2 treatment increased the pSTAT5 level in CXCR5$^+$ T_{PEX} cells but not in CXCR5$^-$ T_{PEX} cells (**Figure 3C**). To directly test the impact of STAT5 signaling, we transduced CD45.2 TCR transgenic P14 T cells that are specific for the LCMV GP_{33-41} epitope with the retrovirus expressing a constitutively activated version of STAT5b (STAT5b-CA) or an empty viral vector control (Johnston et al., 2012). Transduced P14 T cells were then transferred into congenically marked CD45.1 recipient mice followed by LCMV Docile infection (**Figure 3D**). Similar to the effects of IL-2 treatment and in line with a recent report (Beltra et al Immunity 2023), STAT5b-CA overexpression led to an increase in total P14 cells by about three-fold compared to controls (**Figure 3E**). Importantly, the constitutive activation of the STAT5 signaling in P14 cells favored the generation of CXCR5$^-$ T_{EX} over CXCR5$^+$ T_{PEX} cells *in vivo* (**Figure 3F**).

CXCR5$^+$ T_{FH} cells and CXCR5$^+$ T_{PEX} cells share a similar transcriptional program for their generation whereby both are promoted by transcription factors TCF1 and BCL6 and suppressed by BLIMP1 and ID2 (Kallies et al., 2020; Vinuesa et al., 2016). We and others previously reported that IL-2/STAT5 signaling induces the expression of B lymphocyte-induced maturation protein-1 (BLIMP1, encoded by *Prdm1*), a negative regulator of *Cxcr5* transcription (Johnston et al., 2009; Leong et al., 2016; Xin et al., 2016). We therefore examined the roles of BLIMP1 in regulating the differentiation of CXCR5$^+$ T_{PEX} cells in response to IL-2. First, we generated mixed bone marrow chimeric mice containing cells from mice carrying a T cell-specific ablation of Blimp1 (*Prdm1*$^{flox/flox}$*Lck*^{Cre}) and cells from congenically marked wildtype mice, mixed at a 1:1 ratio. These chimeras were infected with LCMV Docile, treated with IL-2 or PBS from day 10 to day 14 and analyzed on day 15 (**Figure 3G**). As expected, we observed larger proportions of CXCR5$^+$ T_{PEX} cells in BLIMP1-deficient (~30%) compared to control (~15%) CD8$^+$ T cells. Notably, IL-2 treatment further reduced the CXCR5$^+$ T_{PEX} cell percentages from ~15% to ~6% in control CD8$^+$ T cells but did not reduce T_{PEX} cell frequencies in BLIMP1-deficient CD8$^+$ T cells, which remained as ~30% (**Figure 3H**). Taken together, our results indicate that the IL-2-STAT5-BLIMP1 axis plays a critical role in regulating the generation of CXCR5$^+$ T_{PEX} cells in response to IL-2 treatment in chronic infection.

An IL-2 fusion protein regulates the balance of effector and T_{PEX} cell generation

IL-2 fusion proteins that increase the half-life or bioavailability of IL-2 have recently been shown to be promising tools in cancer immunotherapy (Beltra et al., 2023; Codarri Deak et al., 2022; Hashimoto et al., 2022; Tichet et al., 2023). To specifically assess the role of the IL-2-CD122 axis in regulating the generation of T_{PEX} cells, we examined the effects of a novel IL-2 fusion protein, ANV410, that selectively targets CD122. Consistent with the CD122-specific activity, treatment of naïve mice with ANV410 resulted in a dramatic expansion of CD44$^+$ memory CD8$^+$ T cells, and NK cells, without affecting T_{REG} cells (**Suppl. Figure 2**). We next treated mice chronically infected with LCMV Docile (8-12 days post infection), which had received LCMV-specific P14 T cells (Regimen A, **Figure 4A**). Total CD8$^+$ as well as P14 T cells expanded substantially in response to ANV410

(**Figure 4B**). We also observed a significant increase in the percentage and numbers of CX3CR1$^+$ T_{EX} cells (**Figure 4C**), which harbor the highest functional capacity among exhausted T cells (Hudson et al., 2019; Zander et al., 2019). Consistent with this observation, we also found larger numbers of P14 T cells expressing Granzyme B (**Figure 4D**). In contrast, the percentages of T_{PEX} cells in P14 T cells declined while their numbers remained unchanged (**Figure 4E**), which was consistent with the results from IL-2 treatment (**Figure 2E**). To examine the effects of the IL-2 fusion protein on the generation of T_{PEX} cells, we treated mice with ANV410 during the first 5 days post infection (Regimen B, **Figure 4A**). Strikingly, early ANV410 treatment dramatically impaired the expansion of P14 T cells (**Figure 4F**) and abrogated T_{PEX} cell development almost completely both in the P14 and polyclonal PD-1$^+$ CD8 T cell compartment (**Figure 4G, H**), suggesting that increased IL-2 signaling early during infection is detrimental to T_{PEX} cell development and function.

IL-2 treatment reduces CXCR5$^+$ T_{PEX} cells in humans

Finally, we asked whether IL-2 treatment in humans could regulate T_{PEX} cells. We took advantage of immunological profiling data that we previously collected in a clinical trial of low-dose IL-2 therapy in patients with systemic lupus erythematosus (SLE). In this clinical trial, patients were treated with three two-week cycles of 1,000,000 IU recombinant human IL-2 every other day (**Figure 4I**) (He et al., 2016a). The results demonstrated that low-dose IL-2 treatment significantly reduced human CXCR5$^+$ T_{PEX} cells in the blood after three cycles of low-dose IL-2 therapy (**Figure 4J**); this is in agreement with the observation of suppression of CXCR5 expression on CD8$^+$ T cells by IL-2 treatment in the mouse model of LCMV chronic infection (**Figure 2C**). Overall, our data in both mice and humans indicate that increased IL-2 signaling via CD122 during early stages of the infection can impair the generation of T_{PEX} cells, while a short period of therapeutic IL-2 treatment at later stages of the infection increases the differentiation of effector cells from T_{PEX} cells without impacting their self-renewal capacity.

DISCUSSION

Upon chronic antigen exposure, $CD8^+$ T cells upregulate the expression of inhibitory receptors including PD-1. $PD\text{-}1^+$ T cells in chronic infection are heterogenous, containing $TCF1^+$ T_{PEX} cells that undergo self-renewal but also give rise to $TCF1^-$ T_{EX} cells that lack long-term proliferative capacity (He et al., 2016b; Huang et al., 2022; Im et al., 2016; Leong et al., 2016; Utzschneider et al., 2016; Wu et al., 2016). Critically, T_{PEX} cells mediate the proliferative burst in response to PD-1 immune checkpoint inhibition, which induces the differentiation of $CX3CR1^+$ effector-like T_{EX} cells, which display the highest effector function and antiviral activity and closely correlate with positive response to therapeutic ICB in cancer (Hudson et al., 2019; Yan et al., 2018; Zander et al., 2019). Maintaining a balance between self-renewal, effector function and terminal exhaustion underlying by these functional subsets is essential to sustain cytotoxic killing while restraining immunopathology at the same time (Blank et al., 2019; Hashimoto et al., 2018; Kallies et al., 2020; McLane et al., 2019). Our results, together with studies published recently (Beltra et al., 2023; Codarri Deak et al., 2022; Hashimoto et al., 2022; Liu et al., 2021; Ren et al., 2022; Sun et al., 2023) suggest that regulating the T_{EX} and T_{PEX} cell balance is a central role of IL-2 and the downstream STAT5-BLIMP1 axis. Importantly, IL-2 promoted the generation of $CX3CR1^+$ effector-like T_{EX} cells without compromising the self-renewal capacity of T_{PEX} cells.

IL-2 signaling is mediated by both the high affinity receptor IL-2Rα (CD25) and the medium affinity receptor IL-2Rβ (CD122). Their individual contribution, however, is dependent on their respective expression levels as well as the dose of IL-2. We found that treatment with native IL-2 resulted in the upregulation of CD122 and induced feedforward signaling. Consistent with this observation, the IL-2 fusion protein ANV410 that selectively targets CD122 but not CD25 induced the generation of CX3CR1 effector-like T_{EX} cells, overall suggesting that CD122 is the main mediator of IL-2 effects on T_{PEX} cells. These results align well with recent studies, which showed that CD122-dependent signals drive terminal differentiation of $CD8^+$ T cells (Beltra et al., 2016) and CD122-biased IL-2 agonism in the combination with ICB promoted $CD8^+$ T cell effector function (Codarri Deak et al., 2022). Our results, however, do not preclude the possibility that IL-2 treatment can induce signaling through CD25 as reported (Hashimoto et al., 2022). Thus, IL-2 signaling is likely to be context-dependent. This notion is also highlighted by

our data showing that early, in contrast to late, treatment with the IL-2 fusion protein ANV410 abrogated T_{PEX} cell development and impaired the expansion of antigen-specific $CD8^+$ T cells.

Recent advancement in our understanding of the central role of IL-2 in the regulation of $CD8^+$ T cell expansion and function has reinvigorated the enthusiasm for IL-2-based immunotherapy in infection and cancer. Indeed, IL-2 and IL-2 fusion proteins have emerged as powerful modulators that may promote viral clearance or tumor control. Nevertheless, more work is required to understand the impact of IL-2 in a therapeutic setting on the function of T_{PEX} cells and thus the long-term maintenance of $CD8^+$ T cell responses in chronic infection and in cancer. Furthermore, the facts that IL-2 signaling modulated the localization of $CD8^+$ T cells and altered the distribution of viral reservoirs which may have implications for people living with HIV or experiencing EBV active infection. Thus, further work is needed to dissect the therapeutic potential of IL-2. Taken together, the development of IL-2-based immunotherapies should not only target the correct receptor subunit but also consider T cell differentiation state and localization.

Acknowledgments

We acknowledge the Imaging and Cytometry Facility at the John Curtin School of Medical Research, The Australian National University and Flowcores at Monash University and Doherty Institute for technical support. We thank Shane P. Crotty (La Jolla Institute for Immunology) for STAT5b-CA and control vectors, William S Foster and James A. Harker (Imperial College London) for the advice on human studies. We thank ANAVEON for the supply of AN410.

Funding

Australian National Health and Medical Research Council (NHMRC) project GNT1085509 (DY), GNT2004333 (AK) and Leader Fellowship GNT2009554 (DY)

National Natural Science Foundation of China (NSFC) project 82071792 (YW)

Natural Science Foundation of Shandong Province 2021ZDSYS12 (YW)

Swiss National Research Foundation fellowship (PMG)

Author Contributions

Conceptualization: DY and AK

Supervision: DY, AK and ZL

Data curation: YC, PZ, PMG, YAL, JH, YW, FVM, TZ, and JY

Formal analysis: PZ, YC, PMG, YAL, YW and MP

Funding acquisition: DY, AK, PMG and YW

Writing, review and editing: DY, AK, PZ, YC and PMG

Declaration of Interests

The authors declare no conflicts of interests.

Figure legends

Figure 1. IL-2 treatment promotes CD8+ T effector expansion during chronic infection.

(**A**) Schematic showing C57BL/6 mice chronically infected with LCMV Docile and receiving intraperitoneal treatment of 30,000 IU recombinant human IL-2 daily from day 10 to 14 post infection, followed by the analyses on day 15. (**B**) Quantification showing CD4/CD8 ratio and the numbers of $CD8^+$ T cells in the spleen. Cells were gated on $7AAD^-$ $B220^-$ $TCR\beta^+CD8^+$ or $CD4^+$ cells using flow cytometry. (**C**,**D**) Representative FACS plots and statistics showing $CD44^{high}CD62L^{low}$ effector (C) and the expression of Granzyme B (D) in total $CD8^+$ T cells in mice treated with PBS or IL-2. (**E, F**) Representative FACS plots and quantification showing the frequencies and numbers of H-2Db LCMV GP_{33} tetramer-specific $CD8^+$ T cells (E) and the frequencies and numbers of $CXCR5^-TCF1^-$ T_{EX} cells and $CXCR5^+TCF1^+$ T_{PEX} cells. Results are representative of two or three independent experiments (*n* = 4-5/group). Each dot represents one individual mouse. Student's unpaired two-tailed t tests.

Figure 2. IL-2 alters tissue localization of $CD8^+$ T cells and viral reservoirs in chronic infection.

(**A**) C57BL/6 mice were chronically infected with LCMV Docile and received intraperitoneal treatment with IL-2 as in Figure 1A. Representative confocal images (left: low magnification, right: high magnification) and quantification of LCMV infected cells in the spleen. (**B**) C57BL/6 mice chronically infected with LCMV Docile and receiving intraperitoneal treatment of gradient doses of recombinant human IL-2 (10,000 – 100,000 IU) daily from day 10 to 14 post infection, followed by the analyses on day 15. FACS plot showing the gating of T_{FH} and non-T_{FH} cells in $CD4^+$ T cells (left), and quantification of virus-infected ($VL4^+$) T_{FH} and non-T_{FH} cells in each group (right). (**C**, **D**) In the same experiment as (A), histograms showing the expression of CXCR5 on GP_{33} tetramer-specific $CXCR5^+$ $CD8^+$ T cells (C) and representative images (left) and quantification (right) of $CD8^+$ T cells in B-cell follicles (D). (**E**) Representative FACS plots (left) and

quantification (right) showing the expression of CXCR5$^+$ on OT-I CD8$^+$ T cells, co-cultured with splenocytes pulsed with the SINFEKL peptide (1 μM) and indicated cytokines: TGFβ (10 ng/mL), IL-6 (100 ng/mL) and IL-2 (500 I.U./mL). Results are representative of at least two independent experiments. Each dot represents one image count (A, D), one individual mouse (B), or one culture (E). Student's unpaired two-tailed t tests.

Figure 3. An IL-2-STAT5-BLIMP1 axis regulates the balance of effector and T_{PEX} generation.

(**A-C**) C57BL/6 mice were chronically infected with LCMV Docile and received intraperitoneal treatment with IL-2 as in Figure 1A. Quantification of the expression of CD122 and CD25 between CXCR5$^+$ T_{PEX} cells and CXCR5$^-$ T_{EX} cells (A). The comparison of the expression of CD122 and CD25 on CXCR5$^+$ T_{PEX} cells or CXCR5$^-$ T_{EX} cells between PBS treated and IL-2 treated mice (B). The comparison of the expression of pSTAT5 in CXCR5$^+$ T_{PEX} cells or CXCR5$^-$ T_{EX} cells between PBS treated and IL-2 treated mice (C). (**D-F**) Schematic (D) showing the overexpression of constitutive active STAT5b (STAT5b-CA) in P14 cells, followed by the adoptive transfer in congenically marked recipient mice with chronical LCMV Docile infection. Representative FACS plots (left) and quantifications (right) of the frequencies of P14 cells in total CD8$^+$ T cells (E) and the frequencies of CXCR5$^+$ T_{PEX} cells in P14 cells (F). (**G**, **H**) Schematic of the generation of bone marrow chimera mice carrying T cell specific deletion of BLIMP1 (encoded by *Prdm1*), followed with chronic LCMV Docile infection and IL-2 treatment (i.p. 30,000 I.U. daily from day 10 to 14 post-infection) (G). Representative FACS plots and quantifications showing the frequencies of CXCR5$^+$ T_{PEX} cells in CD44$^+$ CD8$^+$ T cells (H). Results are representative of two or three independent experiments (n = 4-5/group). Each dot represents one individual mouse. Student's unpaired two-tailed t tests. N.S., statistically not significant.

Figure 4. An IL-2 fusion protein regulates the balance of effector and T_{PEX} cell generation.

(**A**) Schematic showing P14 T cells being transferred into congenically marked mice, which were subsequently infected with LCMV Docile and treated with ANV410, a CD122-specific IL-2 fusion protein, three times every other day from day 8 to 12 post infection

and analyzed on day 14 post infection (regimen 1, panels B-E) or from day 1 to 5 of infection and analyzed on day 7 post infection (regimen 2, panels F-H). (**B**) Quantifications of total $CD8^+$ T cells (left) or P14 cells (right) on day 14 post infection (regimen 1). (**C**) FACS plot showing the gating strategy for $CX3CR1^+$ T_{EX} cells (left) and quantifications of percentages and numbers of $CX3CR1^+$ T_{EX} cells in P14 cells on day 14 post infection (regimen 1). (**D**) Quantification showing percentages and expression levels of $GzmB^+$ P14 cells on day 14 post infection (regimen 1). (**E**) FACS plots showing the gating strategy for $TCF1^+$ T_{PEX} cells (left) and quantification showing the percentages and numbers of $TCF1^+$ T_{PEX} cells in P14 cells on day 14 post infection (regimen 1). (**F**) Quantification showing the percentages and numbers of P14 cells on day 7 post infection (regimen 2). (**G**) FACS plots showing the gating strategy for $TCF1^+$ T_{PEX} cells (left) and quantification showing the percentages and numbers of $TCF1^+$ T_{PEX} cells in P14 cells on day 7 post infection (regimen 2). (**H**) Quantification showing the percentages and numbers of $TCF1^+$ T_{PEX} cells in endogenous $PD\text{-}1^+$ $CD8^+$ T cells on day 7 post infection (regimen 2). (**I**) Schematic of low-dose IL-2 therapy in patients with systemic lupus erythematosus (SLE). (**J**) Quantification showing the frequencies of $CXCR5^+$ T_{PEX} in peripheral blood $CD8^+$ T cells in consecutive time points (left) or before and after the therapy (right). Each dot represents one individual mouse (B-H) or one individual patient (J). Student's unpaired two-tailed t tests (B-H) and paired two-tailed t test (J).

METHODS

RESOURCE AVAILABILITY

Lead contact

Further information and requests for resources and reagents should be directed to and will be fulfilled by the lead contact, Di Yu (di.yu@uq.edu.au).

Materials availability

This study did not generate new unique reagents.

Data and code availability

RNA-seq data were generated from datasets publicly available at GEO. Accession numbers are listed in the Key resources table. qPCR data, microscopy data, and any additional information required to reanalyse the data reported in this paper are available from the lead contact upon request. This paper does not report original code. Scripts and code utilised in this study are available from the lead contact upon request. Information regarding microglia isolation and sequencing can be addressed to Di Yu (di.yu@uq.edu.au).

EXPERIMENTAL MODEL AND STUDY PARTICIPANT DETAILS

Mice

All mice used in this study were held in SPF (specific pathogen free) animal facilities in The Australian National University, Monash University, University of Melbourne or the Walter and Eliza Hall Institute (WEHI). 6-12 weeks C57BL/6 mice or *Ptprca* (CD45.1) mice were used for *in vivo* and *in vitro* experiments. P14 mice (JAX Tg(TcrLCMV)327Sdz) with the transgenic expression of a TCR specific for LCMV glycoprotein $(GP)_{33\text{-}41}$ were used for adoptive transfer experiment, and OT-I mice are with the transgenic expression of a TCR specific for chicken ovalbumin $(OVA)_{257\text{-}264}$. *Lck*^{Cre} mice *were crossed with Prdm1*$^{flox/flox}$ mice (Kallies et al., 2009). All animal experiment ethics were approved by

the designated Animal Ethics Committee of the institutes that were responsible for animal experiments.

Human data

The details of the prospective, open-label study of low-dose recombinant human IL-2 (rhIL-2) in patients with active SLE was described (He et al., 2016a). Briefly, three cycles of rhIL-2 were administered subcutaneously at a dose of 1 million IU every other day for 2 weeks (a total of 7 doses), followed by a 2-week break. Immunological data in peripheral blood mononuclear cells (PBMCs) were measured at baseline and every 2 weeks thereafter until week 12.

METHOD DETAILS

Viral infection

Lymphocytic choriomeningitis virus (LCMV) Docile was propagated using BHK cell line which was cultured with complete DMEM medium. To study the role of IL-2 treatment in chronic LCMV infection, mice were intravenously (i.v.) infected with 1-2×10^6 PFU (plaque-forming units) of LCMV Docile virus in 100 ul of PBS.

IL-2 and ANV410 treatment

10,000 to 100,000 I.U. (international units) of human rhIL-2 (recombinant human IL-2^{Ser125}, Beijing SL Pharma) were intraperitoneally (i.p.) injected into the mice daily for 5 times from days 10 to 14 post LCMV Docile infection. Mice were sacrificed on day 15 post infection and samples were collected for further examination. ANV410, supplied by Anaveon AG (Basel, Switzerland), is a human IL-2/anti-IL-2 circularly permutated fusion protein which selectively signals through the intermediate affinity IL-2R (IL-2Rβ/γ). For treatment with ANV410, naïve or Docile infected mice were treated with 200 μg/kg body weight three times (every other day in five days).

Generation of bone marrow chimeric mice

Bone marrow (BM) cells were collected from femurs of 6-12 weeks old mice with indicated genotypes. Single cells were prepared by pipetting in complete RPMI media. CD45.1 recipient mouse were lethally irradiated twice with 4.75 gray (Gy) of gamma radiation 4 hours apart. BLIMP1-deficient BM cells (CD45.2) were mixed with wildtype control BM cells (CD45.1/CD45.2) at 1:1 ratio and intravenously transferred into irradiated CD45.1 recipient mouse. As control, BM cells from genotyped wild type littermates (CD45.2) were also mixed with wildtype control BM (CD45.1/CD45.2) and reconstituted in recipient CD45.1 mice. Mice were housed for 6 to 8 weeks to allow hematopoietic reconstitution before infection with LCMV Docile virus.

In vitro induction of CXCR5$^+$ CD8$^+$ cells

For induction of CXCR5$^+$ CD8$^+$ T cells, naïve OT-I cells (CD8$^+$Va2$^+$CD44$^-$CD62L$^+$) were purified (10^4 cells/well) and co-cultured with congenical wildtype splenocytes (10^5 cells/well) in 96-well plates, in the presence of the SINFEKL peptide (1 µM) with indicated cytokines: TGFβ (10 ng/mL), IL-6 (100 ng/mL) and IL-2 (500 I.U./mL~30-50ng/mL).

Retroviral transduction on primary cells

GFP bicistronic retroviral vector containing STAT5b-CA or empty vector as described (Johnston et al., 2012) were used to study the overexpression of STAT5b-CA in primary mouse CD8$^+$ T cells. Retroviruses were generated by transfecting the plasmids into a retrovirus-packaging cell line GPE86 using lipofectamine 2000 reagent (Invitrogen). GFP positive GPE86 were cell sorted to isolate stably transfected cells. Stably transfected GPE86 were then cultured in complete DMEM media for 48 hours before the culture supernatant were collected for the transduction of primary cells. Naïve P14 T cells were purified from CD45.2 TCR transgenic P14 mice and stimulated with plate bound anti-CD3 and anti-CD28 for 48 hours. Activated P14 T cells were spinoculated at 800g for 1 hour at 32°C with the retrovirus supernatants packaged by GPE86 cells. Transduced P14 T cells were rested in fresh cRPMI media containing 20 ng/mL of rmIL-7 for 48 hours. About 6,000 GFP$^+$ P14 T cells were sorted by flow cytometry and intravenously (i.v.) transferred into CD45.1 recipient mouse. One day after adoptive transfer, mice were i.v. infected with LCMV Docile at 10^6 PFU. Mice were culled on day 8 post infection for analyses.

Flow cytometry

Single cells were washed, counted, and stained with Fc-receptor blocking antibodies (clone 2.4G2, 1:100 dilution, BD) for 10 min on ice to block non-specific staining. For surface staining, cells were washed once with PBS containing 2% heat-inactivated fetal bovine serum (FBS, Gibco) and stained in an appropriately diluted antibody solution for at least 30 min at 4 °C. The 7-amino-actinomycin D (7-AAD) (BioLegend) was stained to exclude dead cells. For intracellular staining, Cytofix/Cytoperm (BD) was used as user's guide. For intranuclear staining, Foxp3/Transcription Factor Staining Buffer Set (eBioscience) was used as user's guide. To detect LCMV antigen-specific $CD8^+$ T cells, APC-conjugated H-$2D^b$-GP_{33}-tetramer (produced by Biomolecular Resource Facility at The John Curtin School of Medical Research, The Australian National University). To detect LCMV-infected T cells, purified anti-LCMV nucleoprotein (clone VL4) antibody was labelled with Alexa Fluor (AF) 647 using antibody labelling kit (Invitrogen). Splenocytes from LCMV infected mice were first stained with surface antibodies. After permeabilization by the Cytofix/Cytoperm (BD) kit, labelled AF647-VL4 antibody was incubated with the cells for 30 min at 25 °C. Uninfected splenocytes and VL4 unstained splenocytes were used as negative control. Data were collected on a LSR-II or LSRFortessaTM (BD) and analyzed using FlowJo software.

Immunofluorescence

To visualize LCMV infection and P14 cells in splenic tissues, immunofluorescent staining was performed. The middle section of spleens was cut and submerged immediately in Optimal Cutting Temperature (OCT) compound on dry ice and stored at -80°C. OCT blocks were then sectioned at 5 to 10 μm thickness at -20°C. Sections were blocked with Fc-receptor-blocking antibody (clone 2.4G2, 1:100, BD), followed by staining with primary antibodies. Then sections were washed and stained with secondary antibodies or streptavidin. All steps were performed at 25 °C for 60 min in dark and sections were mounted using Prolong Gold (Invitrogen). Slides were visualized using laser scanning confocal microscopy (Leica SP5) at the John Curtin School of Medical Research.

Quantification of infected cells was performed by automatic counting of cells per area of section using Imaris 9.0 software.

RNA sequencing and bioinformatics analysis

RNA sequencing and bioinformatic analyses to compare the transcriptomes between CXCR5^{-} and CXCR5^{+} P14 cells were described previously (Leong et al., 2016). DESeq2 from Bioconductor software (Love et al., 2014) was used to normalize gene counts in GSE76279 dataset, and the genes were ranked based on -log(adjusted p-value of fold change). The ranked list was introduced to GSEA software (Subramanian et al., 2005) to enrich genes in gene sets of a wide range of databases using a curated version of “msigdb v7.2 symbols”. The normalized counts were also filtered for interleukin receptors to produce a heatmap using pheatmap function in r and to construct a bar chart in GraphPad Prism 9. Multiple unpaired t-tests were used to show the level of significancy.

QUANTIFICATION AND STATISTICAL ANALYSIS

Statistical analysis

All results were analyzed by unpaired or paired and two-tailed student t-test for comparison between two groups or one-way ANOVA for calculating univariate data set with more than two groups by GraphPad Prism 8.0 software, unless otherwise specified. Differences were considered to be statistically significant at $p < 0.05$.

Supplementary Materials

Figure S1-S2.

References

Alfei, F., Kanev, K., Hofmann, M., Wu, M., Ghoneim, H.E., Roelli, P., Utzschneider, D.T., von Hoesslin, M., Cullen, J.G., Fan, Y., et al. (2019). TOX reinforces the phenotype and longevity of exhausted T cells in chronic viral infection. Nature 571, 265-269.

Beltra, J.C., Abdel-Hakeem, M.S., Manne, S., Zhang, Z., Huang, H., Kurachi, M., Su, L., Picton, L., Ngiow, S.F., Muroyama, Y., et al. (2023). Stat5 opposes the transcription factor Tox and rewires exhausted CD8(+) T cells toward durable effector-like states during chronic antigen exposure. Immunity 56, 2699-2718 e2611.

Beltra, J.C., Bourbonnais, S., Bedard, N., Charpentier, T., Boulange, M., Michaud, E., Boufaied, I., Bruneau, J., Shoukry, N.H., Lamarre, A., et al. (2016). IL2Rbeta-dependent signals drive terminal exhaustion and suppress memory development during chronic viral infection. Proc Natl Acad Sci U S A 113, E5444-5453.

Blank, C.U., Haining, W.N., Held, W., Hogan, P.G., Kallies, A., Lugli, E., Lynn, R.C., Philip, M., Rao, A., Restifo, N.P., et al. (2019). Defining 'T cell exhaustion'. Nat Rev Immunol 19, 665-674.

Blattman, J.N., Grayson, J.M., Wherry, E.J., Kaech, S.M., Smith, K.A., and Ahmed, R. (2003). Therapeutic use of IL-2 to enhance antiviral T-cell responses in vivo. Nat Med 9, 540-547.

Boyman, O., and Sprent, J. (2012). The role of interleukin-2 during homeostasis and activation of the immune system. Nat Rev Immunol 12, 180-190.

Codarri Deak, L., Nicolini, V., Hashimoto, M., Karagianni, M., Schwalie, P.C., Lauener, L., Varypataki, E.M., Richard, M., Bommer, E., Sam, J., et al. (2022). PD-1-cis IL-2R agonism yields better effectors from stem-like CD8(+) T cells. Nature 610, 161-172.

Collins, D.R., Hitschfel, J., Urbach, J.M., Mylvaganam, G.H., Ly, N.L., Arshad, U., Racenet, Z.J., Yanez, A.G., Diefenbach, T.J., and Walker, B.D. (2023). Cytolytic CD8(+) T cells infiltrate germinal centers to limit ongoing HIV replication in spontaneous controller lymph nodes. Sci Immunol 8, eade5872.

Dutcher, J.P., Schwartzentruber, D.J., Kaufman, H.L., Agarwala, S.S., Tarhini, A.A., Lowder, J.N., and Atkins, M.B. (2014). High dose interleukin-2 (Aldesleukin) - expert consensus on best management practices-2014. J Immunother Cancer 2, 26.

Eberhardt, C.S., Kissick, H.T., Patel, M.R., Cardenas, M.A., Prokhnevska, N., Obeng, R.C., Nasti, T.H., Griffith, C.C., Im, S.J., Wang, X., et al. (2021). Functional HPV-specific PD-1(+) stem-like CD8 T cells in head and neck cancer. Nature 597, 279-284.

Gabriel, S.S., Tsui, C., Chisanga, D., Weber, F., Llano-Leon, M., Gubser, P.M., Bartholin, L., Souza-Fonseca-Guimaraes, F., Huntington, N.D., Shi, W., et al. (2021). Transforming growth factor-beta-regulated mTOR activity preserves cellular metabolism to maintain long-term T cell responses in chronic infection. Immunity 54, 1698-1714 e1695.

Gautam, S., Fioravanti, J., Zhu, W., Le Gall, J.B., Brohawn, P., Lacey, N.E., Hu, J., Hocker, J.D., Hawk, N.V., Kapoor, V., et al. (2019). The transcription factor c-Myb regulates CD8(+) T cell stemness and antitumor immunity. Nat Immunol 20, 337-349.

Hashimoto, M., Araki, K., Cardenas, M.A., Li, P., Jadhav, R.R., Kissick, H.T., Hudson, W.H., McGuire, D.J., Obeng, R.C., Wieland, A., et al. (2022). PD-1 combination therapy with IL-2 modifies CD8(+) T cell exhaustion program. Nature 610, 173-181.

Hashimoto, M., Kamphorst, A.O., Im, S.J., Kissick, H.T., Pillai, R.N., Ramalingam, S.S., Araki, K., and Ahmed, R. (2018). CD8 T Cell Exhaustion in Chronic Infection and Cancer: Opportunities for Interventions. Annu Rev Med 69, 301-318.

He, J., Zhang, X., Wei, Y., Sun, X., Chen, Y., Deng, J., Jin, Y., Gan, Y., Hu, X., Jia, R., et al. (2016a). Low-dose interleukin-2 treatment selectively modulates CD4(+) T cell subsets in patients with systemic lupus erythematosus. Nat Med 22, 991-993.

He, R., Hou, S., Liu, C., Zhang, A., Bai, Q., Han, M., Yang, Y., Wei, G., Shen, T., Yang, X., et al. (2016b). Follicular CXCR5- expressing CD8(+) T cells curtail chronic viral infection. Nature 537, 412-428.

Hu, Y., Hudson, W.H., Kissick, H.T., Medina, C.B., Baptista, A.P., Ma, C., Liao, W., Germain, R.N., Turley, S.J., Zhang, N., et al. (2022). TGF-beta regulates the stem-like state of PD-1+ TCF-1+ virus-specific CD8 T cells during chronic infection. J Exp Med 219.

Huang, Q., Wu, X., Wang, Z., Chen, X., Wang, L., Lu, Y., Xiong, D., Liu, Q., Tian, Y., Lin, H., et al. (2022). The primordial differentiation of tumor-specific memory CD8(+) T cells as bona fide responders to PD-1/PD-L1 blockade in draining lymph nodes. Cell 185, 4049-4066 e4025.

Hudson, W.H., Gensheimer, J., Hashimoto, M., Wieland, A., Valanparambil, R.M., Li, P., Lin, J.X., Konieczny, B.T., Im, S.J., Freeman, G.J., et al. (2019). Proliferating Transitory T Cells with an Effector-like Transcriptional Signature Emerge from PD-1(+) Stem-like CD8(+) T Cells during Chronic Infection. Immunity 51, 1043-1058 e1044.

Humblet-Baron, S., Franckaert, D., Dooley, J., Bornschein, S., Cauwe, B., Schonefeldt, S., Bossuyt, X., Matthys, P., Baron, F., Wouters, C., et al. (2016). IL-2 consumption by highly activated CD8 T cells induces regulatory T-cell dysfunction in patients with hemophagocytic lymphohistiocytosis. J Allergy Clin Immunol 138, 200-209 e208.

Im, S.J., Hashimoto, M., Gerner, M.Y., Lee, J., Kissick, H.T., Burger, M.C., Shan, Q., Hale, J.S., Lee, J., Nasti, T.H., et al. (2016). Defining CD8+ T cells that provide the proliferative burst after PD-1 therapy. Nature 537, 417-421.

Johnston, R.J., Choi, Y.S., Diamond, J.A., Yang, J.A., and Crotty, S. (2012). STAT5 is a potent negative regulator of TFH cell differentiation. J Exp Med 209, 243-250.

Johnston, R.J., Poholek, A.C., DiToro, D., Yusuf, I., Eto, D., Barnett, B., Dent, A.L., Craft, J., and Crotty, S. (2009). Bcl6 and Blimp-1 are reciprocal and antagonistic regulators of T follicular helper cell differentiation. Science 325, 1006-1010.

Kallies, A., Xin, A., Belz, G.T., and Nutt, S.L. (2009). Blimp-1 transcription factor is required for the differentiation of effector CD8+ T cells and memory responses. Immunity 31, 283-295.

Kallies, A., Zehn, D., and Utzschneider, D.T. (2020). Precursor exhausted T cells: key to successful immunotherapy? Nat Rev Immunol 20, 128-136.

Khan, O., Giles, J.R., McDonald, S., Manne, S., Ngiow, S.F., Patel, K.P., Werner, M.T., Huang, A.C., Alexander, K.A., Wu, J.E., et al. (2019). TOX transcriptionally and epigenetically programs CD8(+) T cell exhaustion. Nature 571, 211-218.

Kunz, S., Sevilla, N., McGavern, D.B., Campbell, K.P., and Oldstone, M.B. (2001). Molecular analysis of the interaction of LCMV with its cellular receptor [alpha]-dystroglycan. J Cell Biol 155, 301-310.

Leong, Y.A., Chen, Y., Ong, H.S., Wu, D., Man, K., Deleage, C., Minnich, M., Meckiff, B.J., Wei, Y., Hou, Z., et al. (2016). CXCR5(+) follicular cytotoxic T cells control viral infection in B cell follicles. Nat Immunol 17, 1187-1196.

Liu, Y., Zhou, N., Zhou, L., Wang, J., Zhou, Y., Zhang, T., Fang, Y., Deng, J., Gao, Y., Liang, X., et al. (2021). IL-2 regulates tumor-reactive CD8(+) T cell exhaustion by activating the aryl hydrocarbon receptor. Nat Immunol 22, 358-369.

Love, M.I., Huber, W., and Anders, S. (2014). Moderated estimation of fold change and dispersion for RNA-seq data with DESeq2. Genome Biol 15, 550.

Ma, C., Wang, L., Liao, W., Liu, Y., Mishra, S., Li, G., Zhang, X., Qiu, Y., Lu, Q., and Zhang, N. (2022). TGF-beta promotes stem-like T cells via enforcing their lymphoid tissue retention. J Exp Med 219.

Man, K., Gabriel, S.S., Liao, Y., Gloury, R., Preston, S., Henstridge, D.C., Pellegrini, M., Zehn, D., Berberich-Siebelt, F., Febbraio, M.A., et al. (2017). Transcription Factor IRF4 Promotes CD8(+) T Cell Exhaustion and Limits the Development of Memory-like T Cells during Chronic Infection. Immunity 47, 1129-1141 e1125.

Martinez, G.J., Pereira, R.M., Aijo, T., Kim, E.Y., Marangoni, F., Pipkin, M.E., Togher, S., Heissmeyer, V., Zhang, Y.C., Crotty, S., et al. (2015). The transcription factor NFAT promotes exhaustion of activated CD8(+) T cells. Immunity 42, 265-278.

Marx, A.F., Kallert, S.M., Brunner, T.M., Villegas, J.A., Geier, F., Fixemer, J., Abreu-Mota, T., Reuther, P., Bonilla, W.V., Fadejeva, J., et al. (2023). The alarmin interleukin-33 promotes the expansion and preserves the stemness of Tcf-1(+) CD8(+) T cells in chronic viral infection. Immunity 56, 813-828 e810.

McLane, L.M., Abdel-Hakeem, M.S., and Wherry, E.J. (2019). CD8 T Cell Exhaustion During Chronic Viral Infection and Cancer. Annu Rev Immunol 37, 457-495.

Mylvaganam, G.H., Rios, D., Abdelaal, H.M., Iyer, S., Tharp, G., Mavigner, M., Hicks, S., Chahroudi, A., Ahmed, R., Bosinger, S.E., et al. (2017). Dynamics of SIV-specific

CXCR5+ CD8 T cells during chronic SIV infection. Proc Natl Acad Sci U S A 114, 1976-1981.

Oldstone, M.B., and Campbell, K.P. (2011). Decoding arenavirus pathogenesis: essential roles for alpha-dystroglycan-virus interactions and the immune response. Virology 411, 170-179.

Petrovas, C., Ferrando-Martinez, S., Gerner, M.Y., Casazza, J.P., Pegu, A., Deleage, C., Cooper, A., Hataye, J., Andrews, S., Ambrozak, D., et al. (2017). Follicular CD8 T cells accumulate in HIV infection and can kill infected cells in vitro via bispecific antibodies. Sci Transl Med 9.

Ren, Z., Zhang, A., Sun, Z., Liang, Y., Ye, J., Qiao, J., Li, B., and Fu, Y.X. (2022). Selective delivery of low-affinity IL-2 to PD-1+ T cells rejuvenates antitumor immunity with reduced toxicity. J Clin Invest 132.

Scott, A.C., Dundar, F., Zumbo, P., Chandran, S.S., Klebanoff, C.A., Shakiba, M., Trivedi, P., Menocal, L., Appleby, H., Camara, S., et al. (2019). TOX is a critical regulator of tumour-specific T cell differentiation. Nature 571, 270-274.

Seo, H., Chen, J., Gonzalez-Avalos, E., Samaniego-Castruita, D., Das, A., Wang, Y.H., Lopez-Moyado, I.F., Georges, R.O., Zhang, W., Onodera, A., et al. (2019). TOX and TOX2 transcription factors cooperate with NR4A transcription factors to impose CD8(+) T cell exhaustion. Proc Natl Acad Sci U S A 116, 12410-12415.

Siddiqui, I., Schaeuble, K., Chennupati, V., Fuertes Marraco, S.A., Calderon-Copete, S., Pais Ferreira, D., Carmona, S.J., Scarpellino, L., Gfeller, D., Pradervand, S., et al. (2019). Intratumoral Tcf1(+)PD-1(+)CD8(+) T Cells with Stem-like Properties Promote Tumor Control in Response to Vaccination and Checkpoint Blockade Immunotherapy. Immunity 50, 195-211 e110.

Subramanian, A., Tamayo, P., Mootha, V.K., Mukherjee, S., Ebert, B.L., Gillette, M.A., Paulovich, A., Pomeroy, S.L., Golub, T.R., Lander, E.S., et al. (2005). Gene set enrichment analysis: a knowledge-based approach for interpreting genome-wide expression profiles. Proc Natl Acad Sci U S A 102, 15545-15550.

Sun, Q., Cai, D., Liu, D., Zhao, X., Li, R., Xu, W., Xie, B., Gou, M., Wei, K., Li, Y., et al. (2023). BCL6 promotes a stem-like CD8(+) T cell program in cancer via antagonizing BLIMP1. Sci Immunol 8, eadh1306.

Tichet, M., Wullschleger, S., Chryplewicz, A., Fournier, N., Marcone, R., Kauzlaric, A., Homicsko, K., Deak, L.C., Umana, P., Klein, C., et al. (2023). Bispecific PD1-IL2v and anti-PD-L1 break tumor immunity resistance by enhancing stem-like tumor-reactive CD8(+) T cells and reprogramming macrophages. Immunity 56, 162-179 e166.

Tsui, C., Kretschmer, L., Rapelius, S., Gabriel, S.S., Chisanga, D., Knopper, K., Utzschneider, D.T., Nussing, S., Liao, Y., Mason, T., et al. (2022). MYB orchestrates T cell exhaustion and response to checkpoint inhibition. Nature 609, 354-360.

Utzschneider, D.T., Charmoy, M., Chennupati, V., Pousse, L., Ferreira, D.P., Calderon-Copete, S., Danilo, M., Alfei, F., Hofmann, M., Wieland, D., et al. (2016). T Cell Factor 1-Expressing Memory-like CD8(+) T Cells Sustain the Immune Response to Chronic Viral Infections. Immunity 45, 415-427.

Vinuesa, C.G., Linterman, M.A., Yu, D., and MacLennan, I.C. (2016). Follicular Helper T Cells. Annu Rev Immunol 34, 335-368.

West, E.E., Jin, H.T., Rasheed, A.U., Penaloza-Macmaster, P., Ha, S.J., Tan, W.G., Youngblood, B., Freeman, G.J., Smith, K.A., and Ahmed, R. (2013). PD-L1 blockade synergizes with IL-2 therapy in reinvigorating exhausted T cells. J Clin Invest 123, 2604-2615.

Wu, T., Ji, Y., Moseman, E.A., Xu, H.C., Manglani, M., Kirby, M., Anderson, S.M., Handon, R., Kenyon, E., Elkahloun, A., et al. (2016). The TCF1-Bcl6 axis counteracts type I interferon to repress exhaustion and maintain T cell stemness. Sci Immunol 1.

Xin, A., Masson, F., Liao, Y., Preston, S., Guan, T., Gloury, R., Olshansky, M., Lin, J.X., Li, P., Speed, T.P., et al. (2016). A molecular threshold for effector CD8(+) T cell differentiation controlled by transcription factors Blimp-1 and T-bet. Nat Immunol 17, 422-432.

Yan, Y., Cao, S., Liu, X., Harrington, S.M., Bindeman, W.E., Adjei, A.A., Jang, J.S., Jen, J., Li, Y., Chanana, P., et al. (2018). CX3CR1 identifies PD-1 therapy-responsive CD8+ T cells that withstand chemotherapy during cancer chemoimmunotherapy. JCI Insight 3.

Yao, C., Sun, H.W., Lacey, N.E., Ji, Y., Moseman, E.A., Shih, H.Y., Heuston, E.F., Kirby, M., Anderson, S., Cheng, J., et al. (2019). Single-cell RNA-seq reveals TOX as a key regulator of CD8(+) T cell persistence in chronic infection. Nat Immunol 20, 890-901.

Yu, D., Walker, L.S.K., Liu, Z., Linterman, M.A., and Li, Z. (2022). Targeting T(FH) cells in human diseases and vaccination: rationale and practice. Nat Immunol 23, 1157-1168.

Yu, D., and Ye, L. (2018). A Portrait of CXCR5(+) Follicular Cytotoxic CD8(+) T cells. Trends Immunol 39, 965-979.

Zander, R., Kasmani, M.Y., Chen, Y., Topchyan, P., Shen, J., Zheng, S., Burns, R., Ingram, J., Cui, C., Joshi, N., et al. (2022). Tfh-cell-derived interleukin 21 sustains effector CD8(+) T cell responses during chronic viral infection. Immunity 55, 475-493 e475.

Zander, R., Schauder, D., Xin, G., Nguyen, C., Wu, X., Zajac, A., and Cui, W. (2019). CD4(+) T Cell Help Is Required for the Formation of a Cytolytic CD8(+) T Cell Subset that Protects against Chronic Infection and Cancer. Immunity 51, 1028-1042 e1024.

Zhou, P., Chen, J., He, J., Zheng, T., Yunis, J., Makota, V., Alexandre, Y.O., Gong, F., Zhang, X., Xie, W., et al. (2021). Low-dose IL-2 therapy invigorates CD8+ T cells for viral control in systemic lupus erythematosus. PLoS Pathog 17, e1009858.

Figure 1.

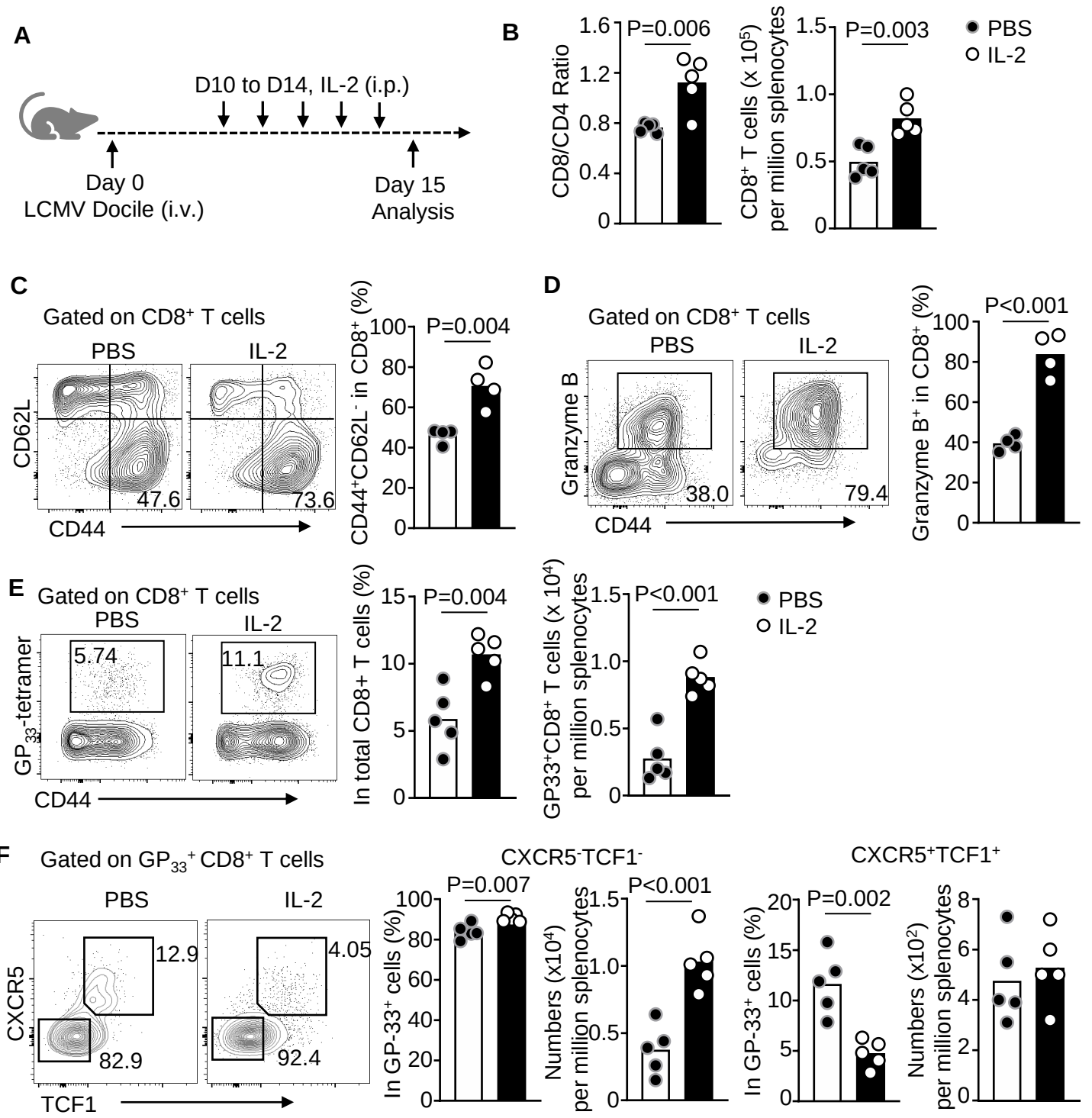
A
D10 to D14, IL-2 (i.p.)
Day 0
LCMV Docile (i.v.)
Day 15
Analysis
B
CD8/CD4 Ratio
P=0.006
CD8+ T cells (x 10^5) per million splenocytes
P=0.003
PBS
IL-2
C
Gated on CD8+ T cells
PBS
IL-2
CD62L
CD44
47.6
73.6
CD44+CD62L- in CD8+ (%)
P=0.004
D
Gated on CD8+ T cells
PBS
IL-2
Granzyme B
CD44
38.0
79.4
Granzyme B+ in CD8+ (%)
P<0.001
E
Gated on CD8+ T cells
PBS
IL-2
GP33-tetramer
CD44
5.74
11.1
In total CD8+ T cells (%)
P=0.004
GP33+CD8+ T cells (x 10^4) per million splenocytes
P<0.001
PBS
IL-2
F
Gated on GP33+ CD8+ T cells
PBS
IL-2
CXCR5
TCF1
12.9
82.9
4.05
92.4
CXCR5-TCF1-
In GP-33+ cells (%)
P=0.007
Numbers (x10^4) per million splenocytes
P<0.001
CXCR5+TCF1+
In GP-33+ cells (%)
P=0.002
Numbers (x10^2) per million splenocytes

Figure 2.

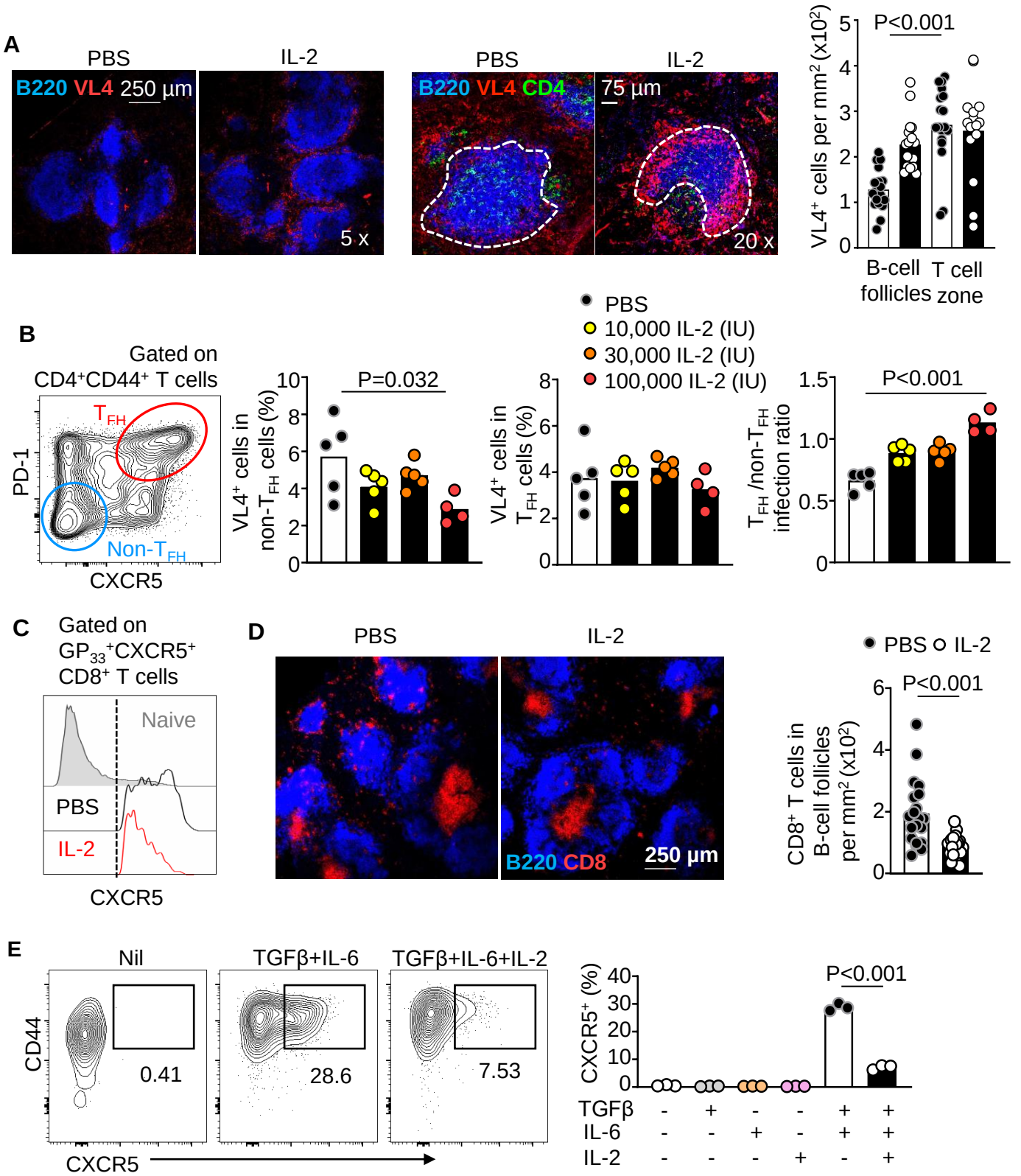
A
PBS
IL-2
B220 VL4 250 µm
5 x
PBS
IL-2
B220 VL4 CD4
75 µm
20 x
VL4+ cells per mm2 (x10^2)
P<0.001
B-cell follicles
T cell zone
B
Gated on CD4+CD44+ T cells
TFH
Non-TFH
PD-1
CXCR5
VL4+ cells in non-TFH cells (%)
P=0.032
PBS
10,000 IL-2 (IU)
30,000 IL-2 (IU)
100,000 IL-2 (IU)
VL4+ cells in TFH cells (%)
TFH /non-TFH infection ratio
P<0.001
C
Gated on GP33+CXCR5+ CD8+ T cells
Naive
PBS
IL-2
CXCR5
D
PBS
IL-2
B220 CD8
250 µm
PBS IL-2
P<0.001
CD8+ T cells in B-cell follicles per mm2 (x10^2)
E
Nil
TGFβ+IL-6
TGFβ+IL-6+IL-2
CD44
0.41
28.6
7.53
CXCR5
CXCR5+ (%)
P<0.001
TGFβ - + - - + +
IL-6 - - + - + +
IL-2 - - - + - +

Figure 3.

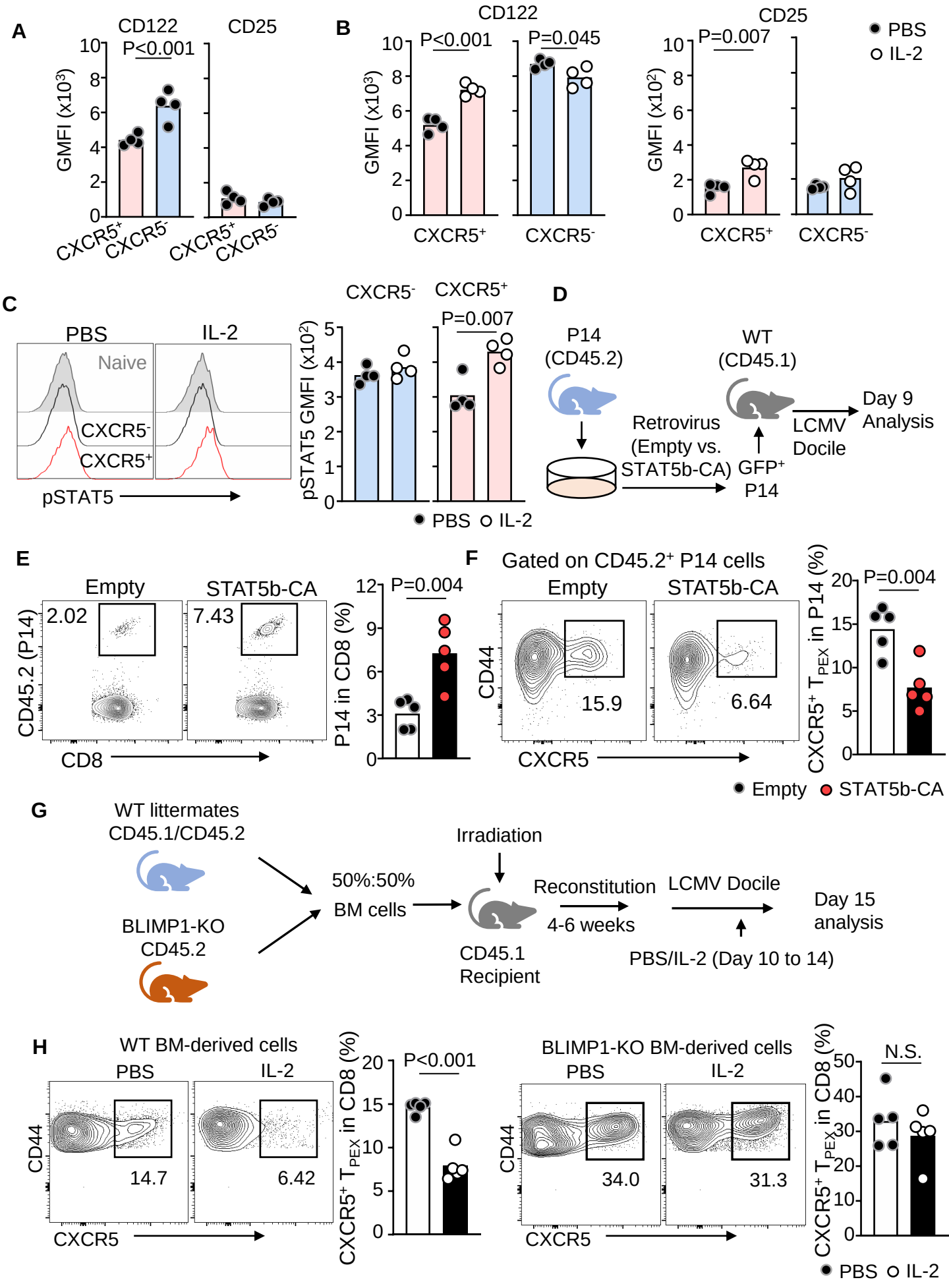
A
CD122
CD25
P<0.001
GMFI (x10³)
CXCR5⁺
CXCR5⁻
B
CD122
CD25
P<0.001
P=0.045
P=0.007
GMFI (x10³)
GMFI (x10²)
PBS
IL-2
C
PBS
IL-2
Naive
CXCR5⁻
CXCR5⁺
pSTAT5
pSTAT5 GMFI (x10²)
P=0.007
D
P14
(CD45.2)
WT
(CD45.1)
Retrovirus
(Empty vs.
STAT5b-CA)
GFP⁺
P14
LCMV
Docile
Day 9
Analysis
E
Empty
STAT5b-CA
2.02
7.43
CD45.2 (P14)
CD8
P14 in CD8 (%)
P=0.004
F
Gated on CD45.2⁺ P14 cells
Empty
STAT5b-CA
CD44
CXCR5
15.9
6.64
CXCR5⁺ T_PEX in P14 (%)
P=0.004
Empty
STAT5b-CA
G
WT littermates
CD45.1/CD45.2
BLIMP1-KO
CD45.2
50%:50%
BM cells
Irradiation
CD45.1
Recipient
Reconstitution
4-6 weeks
LCMV Docile
PBS/IL-2 (Day 10 to 14)
Day 15
analysis
H
WT BM-derived cells
PBS
IL-2
CD44
CXCR5
14.7
6.42
CXCR5⁺ T_PEX in CD8 (%)
P<0.001
BLIMP1-KO BM-derived cells
PBS
IL-2
34.0
31.3
N.S.
PBS
IL-2

Figure 4.

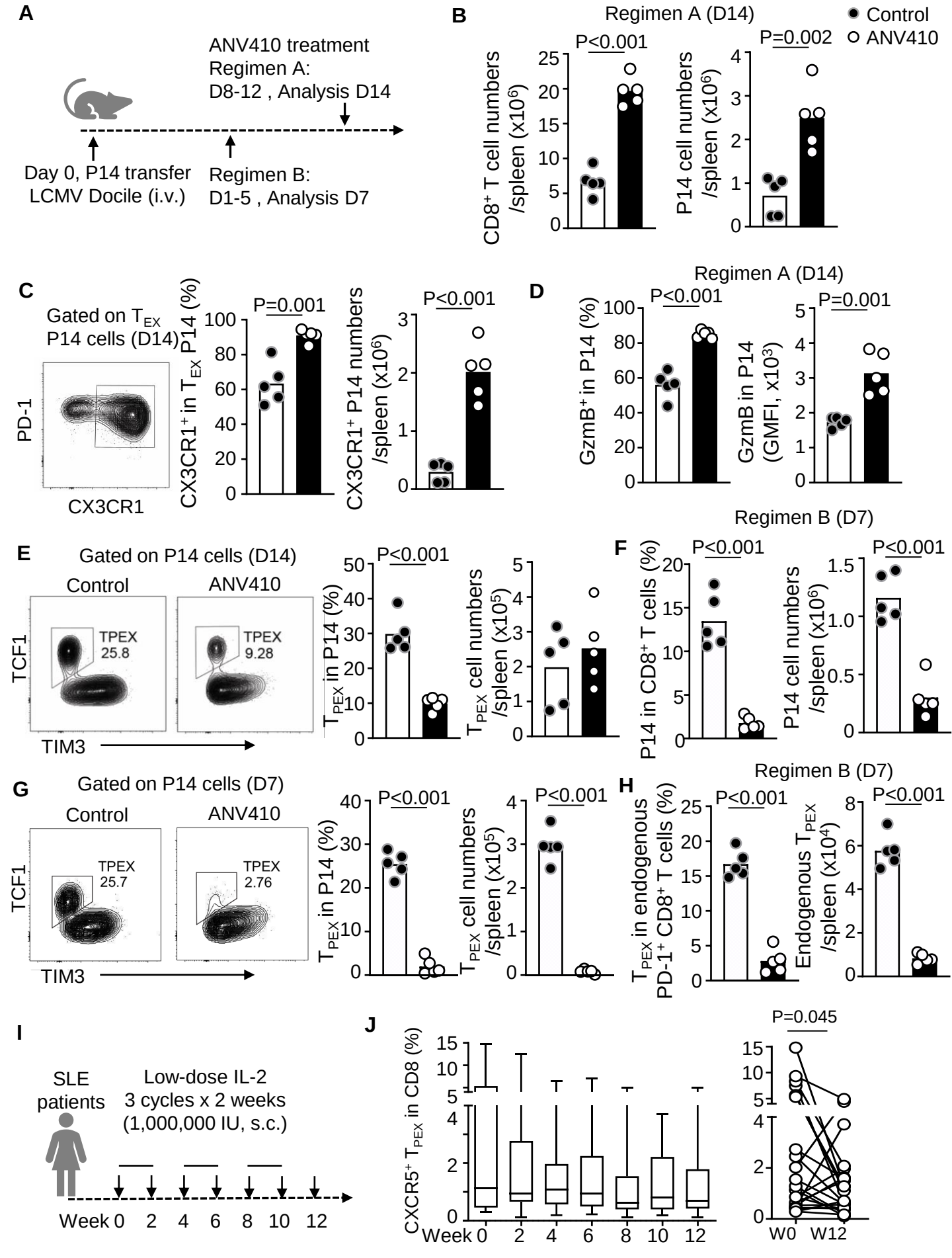
A
ANV410 treatment
Regimen A:
D8-12 , Analysis D14
Day 0, P14 transfer
LCMV Docile (i.v.)
Regimen B:
D1-5 , Analysis D7
B
Regimen A (D14)
Control
ANV410
P<0.001
P=0.002
CD8+ T cell numbers /spleen (x10^6)
P14 cell numbers /spleen (x10^6)
C
Gated on TEX P14 cells (D14)
PD-1
CX3CR1
P=0.001
P<0.001
CX3CR1+ in TEX P14 (%)
CX3CR1+ P14 numbers /spleen (x10^6)
D
Regimen A (D14)
P<0.001
P=0.001
GzmB+ in P14 (%)
GzmB in P14 (GMFI, x10^3)
E
Gated on P14 cells (D14)
Control
ANV410
TCF1
TIM3
TPEX 25.8
TPEX 9.28
P<0.001
TPEX in P14 (%)
TPEX cell numbers /spleen (x10^5)
F
Regimen B (D7)
P<0.001
P<0.001
P14 in CD8+ T cells (%)
P14 cell numbers /spleen (x10^6)
G
Gated on P14 cells (D7)
Control
ANV410
TCF1
TIM3
TPEX 25.7
TPEX 2.76
P<0.001
P<0.001
TPEX in P14 (%)
TPEX cell numbers /spleen (x10^5)
H
Regimen B (D7)
P<0.001
P<0.001
TPEX in endogenous PD-1+ CD8+ T cells (%)
Endogenous TPEX /spleen (x10^4)
I
SLE patients
Low-dose IL-2
3 cycles x 2 weeks
(1,000,000 IU, s.c.)
Week 0 2 4 6 8 10 12
J
P=0.045
CXCR5+ TPEX in CD8 (%)
Week 0 2 4 6 8 10 12
W0 W12

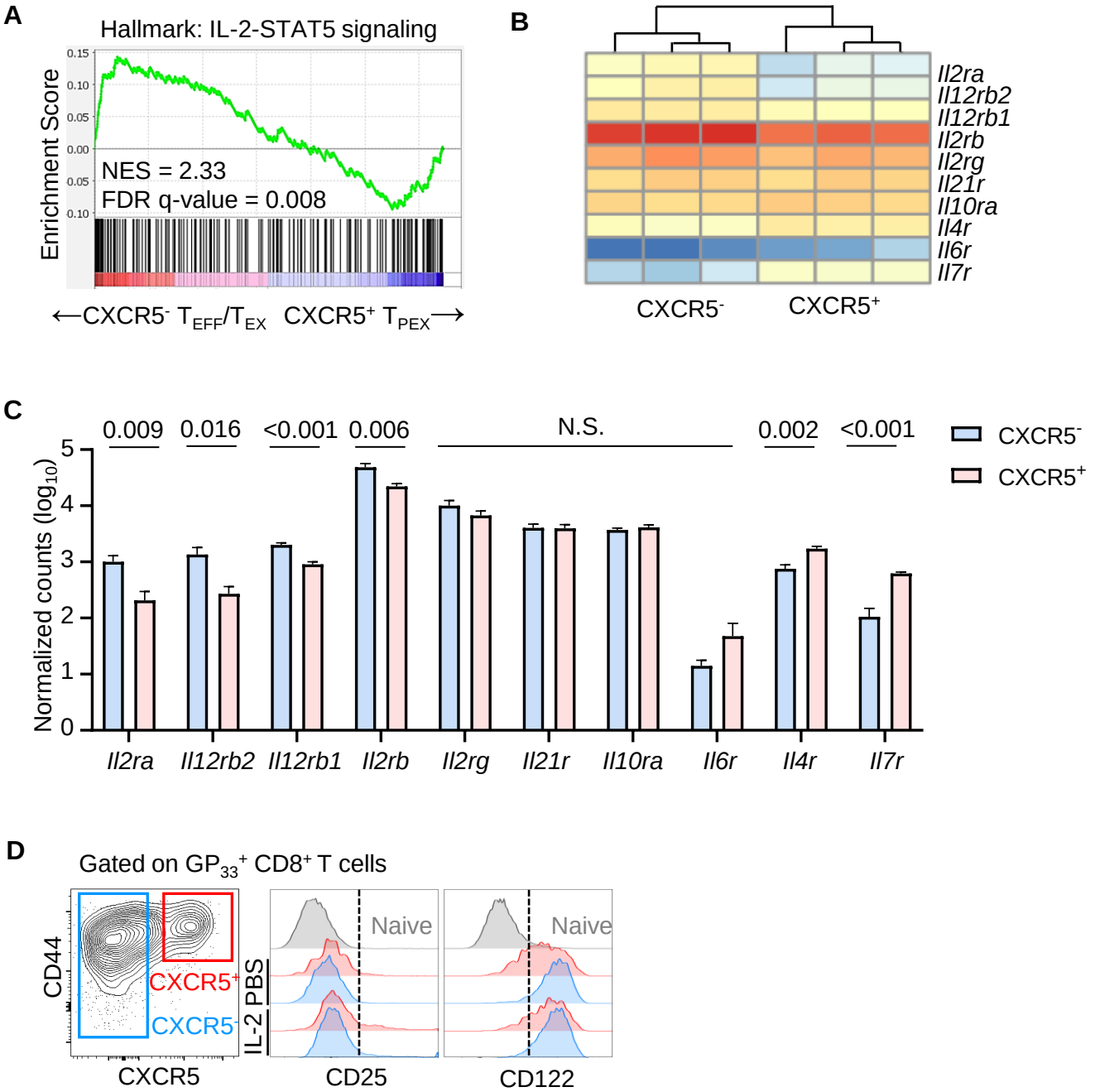

Suppl. Figure 1. Comparison of IL-2-STAT5 signaling and IL-2 receptors between CXCR5⁺ T_{PEX} cells and CXCR5⁻ T_{EX} cells.

(**A-C**) Purified CXCR5⁺ T_{PEX} and CXCR5⁻ T_{EX} P14 cells from host C57BL/6 mice at day 8 post LCMV (DOCILE) infection underwent RNA-seq to generate transcriptomes as described previously (Leong et al., 2016). Gene set enrichment analyses showing the downregulation of IL-2-STAT5 signalling in CXCR5+ T_{PEX} cells (A). Heatmaps (B) and quantification (C) showing the expression of indicated cytokine receptor genes.

(**D**) C57BL/6 mice were chronically infected with LCMV Docile and receiving intraperitoneal treatment of IL-2 as in Figure 1A. FACS plots showing the gating of CXCR5⁺ T_{PEX} cells and CXCR5⁻ T_{EX} populations in LCMV-specific GP_{33} tetramer⁺ CD8⁺ T cells (left) and histograms showing the expression of CD122 and CD25 on indicated populations.

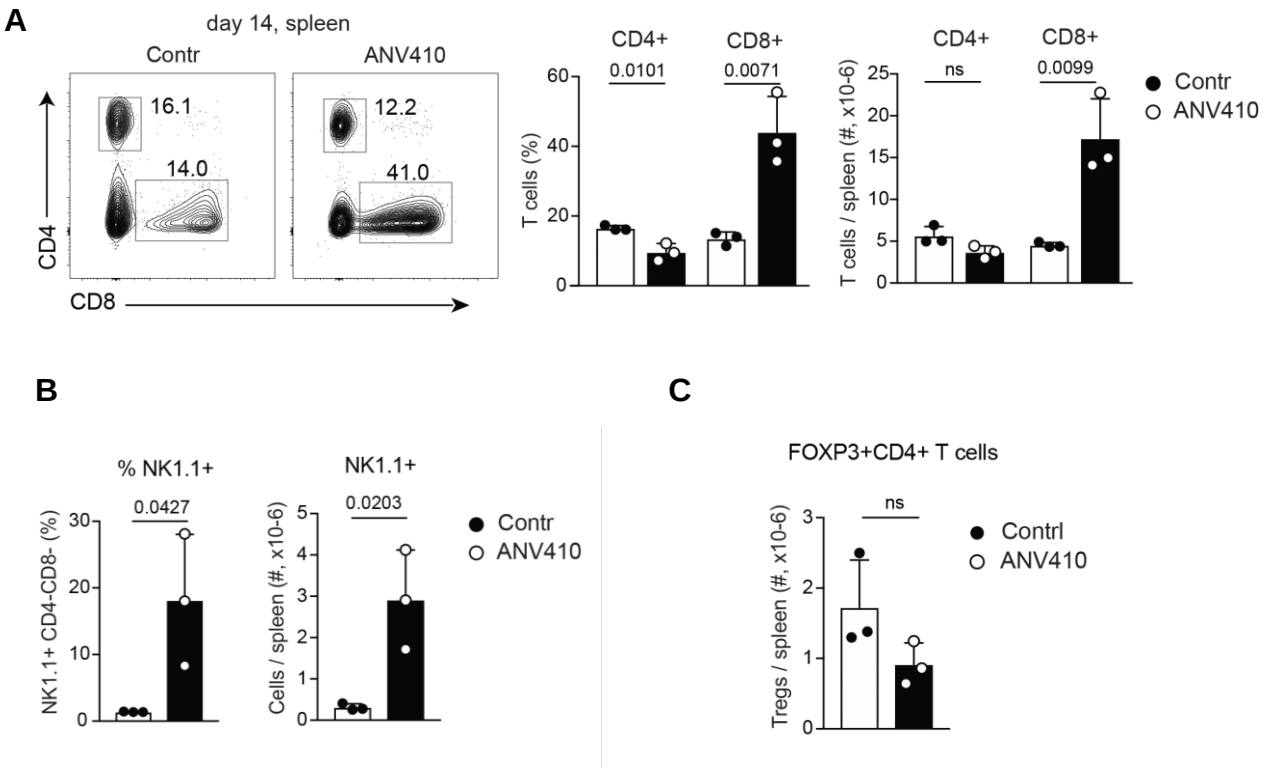

Suppl. Figure 2. Treatment with a CD122-specific IL-2 fusion protein results in CD8 T cell and NK cell but not T_{REG} cell expansion.

C57BL/6 mice were chronically infected with LCMV Docile and receiving intraperitoneal treatment of ANV410 as in Figure 4A (Regimen A).

(**A**) FACS plots (left) and quantifications (right) for total $CD4^+$ or $CD8^+$ T cells.

(**B**) Quantification for $CD3^-NK1.1^+$ NK cells.

(**C**) Quantification for $Foxp3^+$ $CD4^+$ T_{REG} cells.